CrystEngComm

PAPER

View Article Online
View Journal | View Issue



Cite this: *CrystEngComm*, 2022, **24**, 4201

# Hierarchical study of mono- and multicharged imidazolium encapsulation in *p*-sulfonatocalix[4]arene molecular capsules†

Irene Ling, *[a] Cameron L. Campbell, [b] Alexandre N. Sobolev[c] and Scott J. Dalgarno *[b]

Received 31st March 2022,
Accepted 13th May 2022

DOI: 10.1039/d2ce00459c

rsc.li/crystengcomm

Four ternary multi-component crystal structures comprising water-soluble *p*-sulfonatocalix[4]arene anion as the cavitand in the presence of different types of positively charged guest molecules comprising 1-butylimidazolium, 3,3′-(1,4-phenylenebis(methylene))bis(1-methylimidazolium), 3,3′,3″-(benzene-1,3,5-triyltris(methylene))tris(1-methylimidazolium), or 3,3′,3″,3‴-(benzene-1,2,4,5-tetrayltetrakis(methylene))-tetrakis(1-methylimidazolium) and aquated lanthanide(III) ions (Gd(III) or Ce(III)) are reported. Careful crystallographic analysis shows that all positively charged imidazole rings are encapsulated by *p*-sulfonatocalix[4]arene for 1-butylimidazolium and 3,3′-(1,4-phenylenebis(methylene))bis(1-methylimidazolium), however, partial encapsulation was observed for 3,3′,3″-(benzene-1,3,5-triyltris(methylene))tris(1-methylimidazolium) and 3,3′,3″,3‴-(benzene-1,2,4,5-tetrayltetrakis(methylene))-tetrakis(1-methylimidazolium). The formation of a molecular capsule prevails in all structures regardless of the type of guest species. Supermolecules in three of the complexes self-assemble into a bilayer arrangement in the extended structure, whilst those involving *p*-sulfonatocalix[4]arene and 1-butylimidazolium form hydrated channels through alternative packing.



## Introduction

Molecular capsules can be considered as scaffolds with an internal cavity capable of accommodating a suitably sized guest molecule. Understanding the formation of such species is important in the development of nanosized reactors for applications such as catalysis[1] and drug delivery.[2–5] The simplest form of molecule capsule is connecting two cavitands at their open ends, where these are often linked by non-covalent interaction such as hydrogen bonds[6–8] and/or metal-coordination.[9–14] Examples of molecular capsules formed *via* complementary hydrogen bonding interactions include (but are not limited to) glycoluril-based "tennis balls" and "softballs",[15,16] deep cavity octa-acid or resorcin[4]arene-based dimers,[17] and tetrol-[7] and calixpyrrole-based[18] capsules.

Cone-shaped calix[4]arene-based host molecules belong to the class of cavitands and have a long history in the study of molecular recognition.[19,20] Although calixarenes were not as successful as resorcinarenes in the formation of deep-cavity structures, they have shown the ability to form remarkable self-assembled nanoscale capsules with the internal core capable of housing a variety of suitably sized guest molecules.[21] The interactions of the host molecules with the guest vary depending on the functional groups appended to the calix[4]arene scaffold. *p*-Sulfonatocalix[4]arene (SC4), with functional groups at the upper-rim, is an effective water-soluble host molecule that can accommodate a wide range of guest molecules in the hydrophobic cavity.[22] A diverse array of inclusion complexes and structural motifs involving weak non-covalent interactions has been extensively reported, and it was found that SC4s commonly self-assemble into anti-parallel bilayers, with molecular capsules acting as repeat units in the extended structures.[23] To this end, we have investigated the self-assembly of a series of singly and doubly charged *n*-alkylimidazolium-based cations in the presence of SC4 and other auxiliary components such as lanthanides and phosphonium ions, affording a wide range of interesting solid-state assemblies.[22,23] A common feature of these assemblies/crystal structures is that SC4 displays preferential binding towards the positively charged imidazole ring where the five-membered heterocycle is drawn into hydrophobic

[a] *School of Science, Monash University Malaysia, Jalan Lagoon Selatan, 47500 Bandar Sunway, Selangor, Malaysia. E-mail: ireneling@monash.edu*
[b] *Institute of Chemical Sciences, School of Engineering and Physical Sciences, Heriot-Watt University, Riccarton, Edinburgh, UK. E-mail: S.J.Dalgarno@hw.ac.uk*
[c] *School of Molecular Sciences, M310, The University of Western Australia, 35 Stirling Highway, Perth, WA 6009, Australia*

† Electronic supplementary information (ESI) available: Fingerprint plots generated from Hirshfeld surfaces and large versions of figures. CCDC 2127101–2127104. For ESI and crystallographic data in CIF or other electronic format see DOI: https://doi.org/10.1039/d2ce00459c

cavity and stabilised by multiple weak hydrogen bonding and π-stacking interactions.[22,23] It is also noteworthy that the supermolecules consistently form bilayer arrays along with lanthanide metal ions populated in the hydrophilic regions, whilst phosphonium cations occupy the interstices of the hydrophobic layer.[24] This paper is concerned with the objective of expanding the understanding of such inclusion behaviour upon moving to quadruply charged imidazolium cations in the absence of phosphonium salts, with structural studies aimed at providing key insight into host–guest behaviours, inclusion properties, intermolecular interactions, and the overall organisation of the complexes in the crystalline state.

# Experimental

### Synthesis of complexes 1–4

The synthesis of complexes **1–4** (Scheme 1) involves *p*-sulfonatocalix[4]arene tetrasodium salt ($Na_4SC4$), four different imidazolium based salts, and a hydrated lanthanide(III) chloride ($Gd^{3+}$ or $Ce^{3+}$). SC4, 1-methyl-3-butylimidazolium chloride (G1), gadolinium(III) chloride hexahydrate and cerium(III) chloride hexahydrate salts were purchased from Sigma Aldrich and used as received. Imidazolium salts 3,3′-(1,4-phenylenebis-(methylene))bis(1-methylimidazolium) bromide, G2; 3,3′,3″-(benzene-1,3,5-triyltris(methylene))tris(1-methylimidazolium) bromide, G3; 3,3′,3″,3‴-(benzene-1,2,4,5-tetrayltetrakis-(methylene))tetrakis(1-methylimidazolium) bromide, G4; were synthesised according to literature procedures.[25,26] A hot solution of 2 mM SC4 sodium salt and 1 mM imidazolium salt in distilled water (2 mL) was prepared. Three-fold excess of gadolinium(III) chloride hexahydrate or cerium(III) chloride hexahydrate in distilled water (1 mL) was added and mixed thoroughly into the former solution. The solution was left to cool and evaporate slowly at room temperature, with suitable quality crystals for X-ray diffraction studies formed after several days from the saturated solution. Unit cell dimensions of multiple crystals were checked to establish homogeneity of the materials, noting that prolonged removal from the mother liquor results in solvent loss (which is typical for this type of material[27]).

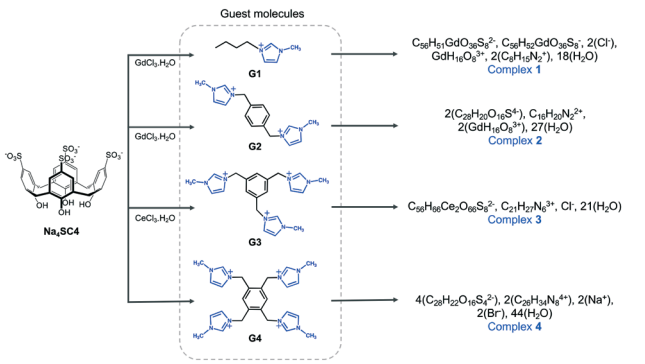


**Scheme 1** Synthesis of inclusion complexes **1** to **4**.

### Structure determinations

All data were measured from single crystals using an Oxford Diffraction Gemini-R Ultra (complex **1**, **2** and **4**) and Bruker X8 Apex II (complex **3**) CCD diffractometers at low temperature with monochromatic CuKα ($\lambda$ = 1.54178 Å) radiation respectively. Data were corrected for Lorentz and polarization effects, and absorption correction applied using multiple symmetry equivalent reflections. The structures were solved by direct methods and refined against $F^2$ with full-matrix least-squares using the program suite SHELX.[28] Anisotropic displacement parameters were employed for the non-hydrogen atoms. Some of the calixarene sulfonate groups exhibit rotational 'disorder' around C–S bonds. Additionally, H-atoms were not successfully located on some disordered waters of crystallisation. Residual electron density in the crystals which could not be interpreted as chemically reasonable moieties (complexes **1** and **4**) was effectively removed by use of the program SQUEEZE.[29] All remaining hydrogen atoms were added at calculated positions and refined using a riding model with isotropic displacement parameters based on those of the parent atom.

# Results and discussion

The structural elucidations of four different multi-component complexes involving SC4 and G1/G2/G3/G4, along with the presence of lanthanide cation ($Gd^{3+}$ or $Ce^{3+}$) have been carefully refined.‡ All four structures have the SC4s acting as ditopic receptors, encapsulating the imidazolium-based guest molecule to form the molecular capsule arrangement at 2 : 1 ratio. The complementarity of electrostatic interaction of the cationic five-membered imidazolium ring and nearest substituents with the calixarene is evident. The availability of

‡ Crystal data for **1** (CCDC 2127101): $C_{128}H_{185}Cl_2Gd_3N_4O_{98}S_{16}$ ($M$ = 4403.40 g mol$^{-1}$), monoclinic, space group $C2$ (no. 5), $a$ = 39.2309(9) Å, $b$ = 16.5501(3) Å, $c$ = 18.5853(4) Å, $\beta$ = 90.788(2)°, $V$ = 12065.8(4) Å$^3$, $Z$ = 2, $T$ = 100(2) K, $D_{calc}$ = 1.212 g cm$^{-3}$, 32 696 reflections measured, $2\theta_{max}$ = 136.0°, 32 698 unique ($R_{int}$ = n/a*) which were used in all calculations. The final $R_1$ was 0.0805 ($I > 2\sigma(I)$) and w$R_2$ was 0.2111 (all data). *Merge of reflections not implemented in the case of refinement of twinned structures.

Crystal data for **2** (CCDC 2127102): $C_{72}H_{146}Gd_2N_4O_{75}S_8$ ($M$ = 2838.90 g mol$^{-1}$), monoclinic, space group $P2_1/c$ (no. 14), $a$ = 18.2391(6) Å, $b$ = 18.4438(3) Å, $c$ = 18.0440(4) Å, $\beta$ = 111.361(3)°, $V$ = 5653.0(3) Å$^3$, $Z$ = 2, $T$ = 100(2) K, $D_{calc}$ = 1.668 g cm$^{-3}$, 58 548 reflections measured, $2\theta_{max}$ = 134.6°, 10 070 unique ($R_{int}$ = 0.0871) which were used in all calculations. The final $R_1$ was 0.0701 ($I > 2\sigma(I)$) and w$R_2$ was 0.1527 (all data).

Crystal data for **3** (CCDC 2127103): $C_{77}H_{135}Ce_2ClN_6O_{66}S_8$ ($M$ = 2773.07 g mol$^{-1}$), triclinic, space group $P\bar{1}$ (no. 2), $a$ = 16.1456(4) Å, $b$ = 18.3448(5) Å, $c$ = 19.8609(5) Å, $\alpha$ = 90.342(1)°, $\beta$ = 102.804(1)°, $\gamma$ = 102.467(1)°, $V$ = 5592.1(3) Å$^3$, $Z$ = 2, $T$ = 198(2) K, $D_{calc}$ = 1.647 g cm$^{-3}$, 140 358 reflections measured, $2\theta_{max}$ = 133.2°, 19 727 unique ($R_{int}$ = 0.0612) which were used in all calculations. The final $R_1$ was 0.0634 ($I > 2\sigma(I)$) and w$R_2$ was 0.1575 (all data).

Crystal data for **4** (CCDC 2127104): $C_{164}H_{244}Br_2N_{16}Na_2O_{108}S_{16}$ ($M$ = 4886.50 g mol$^{-1}$), orthorhombic, space group $C222_1$ (no. 20), $a$ = 18.6967(1) Å, $b$ = 20.4219(2) Å, $c$ = 32.1370(2) Å, $V$ = 12270.62(16) Å$^3$, $Z$ = 2, $T$ = 100(2) K, $D_{calc}$ = 1.323 g cm$^{-3}$, 75 031 reflections measured, $2\theta_{max}$ = 134.5°, 10 927 unique ($R_{int}$ = 0.0684) which were used in all calculations. The final $R_1$ was 0.1581 ($I > 2\sigma(I)$) and w$R_2$ was 0.3555 (all data).

 

these structures has enabled a systematic investigation of the influence of substitution positions at the (methylene)phenyl ring upon the supramolecular host–guest interplay based on various weak intermolecular interactions (*e.g.* hydrogen bonding) and metal coordination. Substituent effects, relative to the positions, are shown to be marked in terms of the ways in which the molecules aggregate to form molecular capsule arrangements and greatly reflect on the size of the capsule (*vide infra*). Additionally, steric considerations for these cations have proven critical in the control of the manner by which host and guest molecules interact; full and partial encapsulation was observed for smaller (G1 and G2) and larger guest molecules (G3 and G4), respectively.

### Structure of $G1^{+}\subset[SC4^{3-}–Gd^{3+}(H_2O)_4–SC4^{2-}][G1^{+}\subset[(SC4^{2-})_2–Gd^{3+}(H_2O)_4][Gd^{3+}(H_2O)_8][Cl^{-}]_2\cdot 18H_2O$, 1

Structure solution of the needle-shaped crystals of **1** was performed in the monoclinic space group *C*2 (*Z* = 2). The moiety formula above represents the structure components together with their charge distribution in the system. The asymmetric unit comprises two SC4 anions in the form of a capsule, one 8-coordinate tetraaqua $Gd^{3+}$ cation (which makes the system polymeric in the crystal), half homoleptic 8-coordinate octaaqua $Gd^{3+}$ cation that is located on a 2-fold axis, one encapsulated G1 monocation, one disordered chloride anion (partial occupancy) and nine waters of crystallisation (some of which are disordered). The formation of a molecular capsule is prevalent in this complex (Fig. 1a) with each assembly shrouding one *n*-butyl methylimidazolium cation and we note such inclusion complex formation is in line previously reported structures (CCDC refcodes: RUZNUX,[30] DUXJUC[31] and DUXKAJ,[31] Fig. 1b). In those cases, the imidazolium cation was confined within the cavities of two opposing calixarenes, albeit the absence of phosphonium cations. Notable differences are observed for complex **1** in comparison to RUZNUX, DUXJUC and DUXKAJ: i) the *n*-butylmethylimidazolium monocation is not disordered, ii) the molecular capsule is slightly skewed to afford a C-shaped (rather than head-to-head) dimer (Fig. 1a), and iii) molecular capsules are not assembled into the common bilayer arrangement typically found for SC4 (Fig. 1c).

Detailed inspection of **1** shows that the confined G1 monocation has its charged head group located deeper into the calixarene cavity, associated with multiple weak interactions that include: (i) C–H···π interaction of methyl group to the SC4 phenyl ring, with C···π distances at 3.64 Å and ii) an H-atom of the imidazole ring has close C–H···O contact with SC4 sulfonate group, with the shortest C–H···O distance at 2.34 Å (corresponding C···O distance 3.18 Å). The SC4 is in a pinched cone conformation in accommodating the *n*-butyl methylimidazolium moiety, with distal phenyl ring pairs splayed and pinched to accommodate the guest (dihedral angles provided in ESI†). The *n*-butyl chain nestles close to an adjacent SC4 upper-rim and forms a weak hydrogen bond to the gadolinium(III) hydration sphere with a C–H···O distance at 2.65 Å. We utilised Hirshfeld surface analysis generated by the

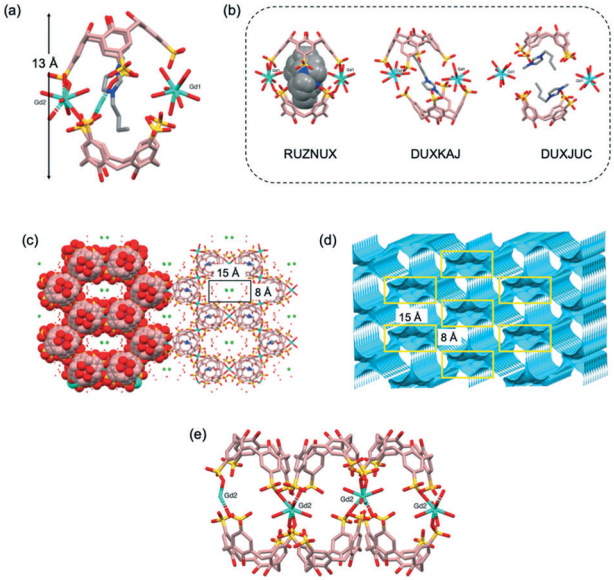


**Fig. 1** (a) Molecular capsule formed in complex **1**. (b) Comparable inclusion complex with complex **1** (RUZNUX,[30] DUXJUC[31] and DUXKAJ[31]). (c) Partial space-filling illustrating the extended packing in complex **1** and (d) hydrophilic channels of 15 Å × 8 Å formed along *c*-axis. (e) Coordination environment for gadolinium(III) connecting four units of SC4s forming an infinite polymeric network. Hydrogen atoms omitted for clarity and figures are not to scale.

CrystalExplorer[32] to further elucidate the intermolecular interactions in complex **1**. Analysis of the two-dimensional fingerprint plot (Fig. S1†) shows that the interplay of G1 and SC4 is stabilised by O···H/H···O (35.0%) and C···H/H···C (37.3%) contacts (corresponding to C–H···π) as these are the major contributors to the Hirshfeld surface of G1 monocation, while reciprocal H···H interaction (van der Waals interactions) contributes 20.6%.

The aquated $Gd^{3+}$ metal ions in complex **1** are an integral part of the cohesion of the C-shaped molecular capsule, and are involved in both primary and secondary coordination interactions to the calixarene sulfonate moieties. The Gd1 metal centre on the two-fold rotation axis is bound by eight water molecules (Gd1–O bond distances in the range of 2.36(1)–2.43(1) Å) and has distorted square antiprismatic geometry. Gd1 is not directly bound to SC4 sulfonate groups, but does form secondary coordination sphere interactions through water ligands to the oxygen donors from opposing calixarene upper-rim sulfonates with O···O distances ranging from 2.68(3)–2.88(4) Å. Gd2 is eight-coordinated, adopts distorted square antiprismatic geometry, is fully occupied and acts as a hinge to connect the four SC4s through direct coordination to the sulfonate groups (O···O distances ranging from 2.56(2)–2.89(2) Å) with the remaining sphere fulfilled by water ligands (Gd2–O distances in the range of 2.344(7)–2.381(7) Å). The size of the capsule is smaller (13 Å, measured between SC4 lower-rim centroids, Fig. 1a) compared to those found in DUXJUC and DUXKAJ (17 Å and 15 Å respectively). In contrast, the capsule in **1** is comparable to that found in RUZNUX, although it is more skewed as shown in Fig. 1b.

The construction of complex **1** is distinctive in the way that the extended structure is built up, with repeating layers of molecular capsules of SC4s and G1 forming a distorted hexagonal array that generates a near-rectangular channel as shown in Fig. 1c and d. Molecular capsules are connected through H-bonding interactions between one another involving metal coordination where each Gd2 metal centre coordinates to four SC4s and forms the infinite polymeric capsular chain (Fig. 1e). Hirshfeld surface analysis shows that intermolecular O···H hydrogen bonding involving the SC4 sulfonate and hydroxyl groups to the adjacent SC4 molecules constitutes further stabilisation to the extended packing with almost 50% contribution to the overall surface, and close O···H contacts in the range of 2.38–2.59 Å. The intermolecular O···H hydrogen bonding is evident from the 2D fingerprint plot as prominent pair of spikes with almost equal lengths (at $d_e + d_i \sim 1.6$ Å) and is indicative for strong hydrogen bonds. The infinite channel in **1** is approx. 15 Å × 8 Å in size (Fig. 1c and d) and is occupied by water molecules and chloride ions, making up ~40% of the unit cell volume. There are some disordered water molecules (with a partial occupancy of 0.50) that are in close proximity to the O-atoms of the SC4 sulfonate groups. These participate in weak interactions amongst themselves and contribute 17.0% to the overall assembly.

### Structure of $[G2^{2+}\subset(SC4^{4-})_2][Gd^{3+}(H_2O)_8]_2\cdot 27H_2O$, 2

Sizable plate-like single crystals of complex **2** were found to crystallise with a monoclinic $P2_1/c$ space group and display dense crystal packing ($D_c$ = 1.668 g cm$^{-3}$). The asymmetric unit comprises one pinched cone SC4 tetraanion, one G2 dication located on an inversion centre, one homoleptic 8-coordinate octaaqua $Gd^{3+}$ cation in the square antiprismatic geometry and 13.5 water molecules. Symmetry expansion gives rise to the formation of a molecular capsule (Fig. 2a), and the interplay of the G2 dication with the calixarene cavities is similar to that found in previously reported complexes based on the same components (CCDC refcodes: OHAMEQ[33] and OHAMIU,[33] Fig. 2b). In all cases the complementarity of electrostatic interactions of the positively charged imidazole ring with SC4 effectively creates molecular capsules made up of two tetra-anionic SC4s from adjacent bilayers. Further inspection of the extended capsule structure in **2** shows that two aquated $Gd^{3+}$ cations are located at the equatorial plane generated by the SC4 upper-rims, bridging these components through extensive hydrogen bonding interactions (O···O distances from 2.751(5)–2.995(5) Å). This supermolecule found in **2** exhibits a close resemblance to OHAMEQ, as judged from the similar interplay of the methylimidazolium groups with the SC4 cavities. The centrosymmetric G2 molecule takes on the *trans*-configuration of the imidazolium groups relative to the central benzene ring (N–C–C = 111.4°, Fig. 2c) and has invoked a skew in the molecular capsule of approximately 11.7° from an axial reference. Nevertheless, the *trans*-G2 in

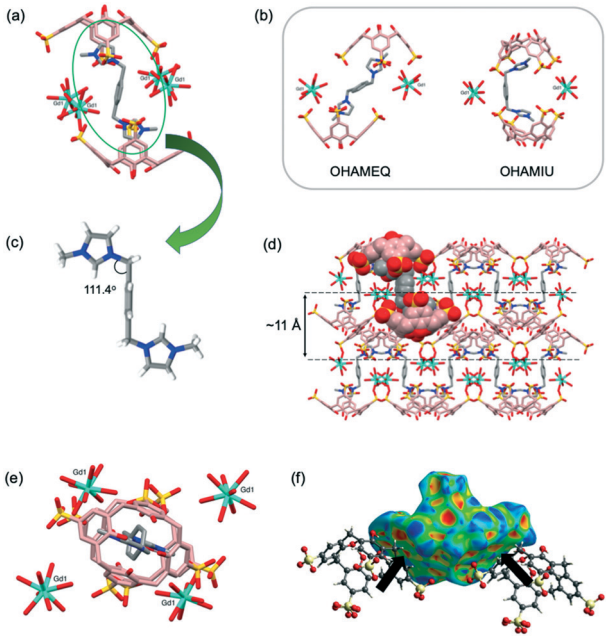


**Fig. 2** (a) Molecular capsule formed in complex **2**. (b) Comparable inclusion complex with complex **2** (OHAMEQ[33] with G2 in *trans*-conformation and OHAMIU[33] with G2 in *cis*-conformation). (c) *trans*-Conformation of G2 encapsulated within the core of the molecular capsule. (d) Partial space-filling illustrating the extended packing in complex **2**. (e) Top view showing gadolinium(III) metal ions surrounding the molecular capsule seam. (f) Hirshfeld surface mapped with shape index to illustrate the π–π interactions evident from the red and blue triangles on the surface. H-Atoms were omitted for clarity except in (c) and (f), and figures are not to scale.

OHAMEQ has larger capsular skew angle (64.3°) owing to the larger bond angle of the imidazolium groups relative to the central benzene ring (107.9°). Although both complex **2** and OHAMEQ have very similar interplay of the *trans*-G2 dication with SC4s, they differ subtly in the orientation of the five membered rings such that the bis-imidazolium species in complex **2** has the symmetry unique methyl group directed towards the SC4 sulfonate groups, with a C···O distance of 3.76 Å. In contrast, G2 in OHAMEQ is oriented such that the methyl group points towards the SC4 hydrophobic cavity, with the C···$\pi_{(centroid)}$ distance of 3.27 Å. The C-atoms at the methylene bridges are in close proximity to the SC4 sulfonate group (C···O distance of 3.41 Å) and the $Gd^{3+}$ hydration sphere (C···O distance of 3.52 Å). The relative contributions of various interactions from the fingerprint plot for the host and guest interplay in complex **2** are shown in Fig. S2† which clearly exhibits the main intermolecular interactions were found to be reciprocal H···H (36.4%) and O···H/H···O (30.2%) contacts.

The extended structure of complex **2** (Fig. 2d) can be regarded as being built from the assembly of molecular capsules and with distinct alternating hydrophobic and hydrophilic layers in which water molecules fill the hydrophilic channels located between the bilayers. Hydrogen bonding is the major contributor to the cohesion of the

 

structure with ~74% contributed reciprocal H···H and O···H/H···O interactions. It is noteworthy that the electrostatics are important in the overall cohesion of complexes (Fig. 2e), however the hydrophobic–hydrophobic interactions also contributed to the overall assembly. Adjacent SC4s form π···π stacking with distance at 3.63 Å and the presence of π–π stacking interactions is further confirmed from the Hirshfeld surface mapped with shape-index where red and blue triangles can be seen on the surface and contribute 4.6% to the overall surface (Fig. 2f). Hirshfeld surface analysis also showed that C···H/H···C interaction (corresponding to C–H···π) is significant for crystal packing where it contributes 16.8% to the overall structure. The thickness of the bilayer is ~11 Å while the distance between the bilayers is ~17 Å; this is defined at the distance between the central plane of one bilayer relative to central plane of the next. Both the bilayer thickness and inter-bilayer distance are relatively short compared to OHAMEQ due to the absence of the phosphonium molecules, showing that complex **2** has a more compact bilayer arrangement.

### Structure of $[G3^{3+}\subset(Ce^{3+}(H_2O)_6{-}(SC4^{4-})_2{-}Ce^{3+}(H_2O)_7)][Cl^-]\cdot 21H_2O$, 3

Complex **3** crystallises in the triclinic $P\bar{1}$ space group and the asymmetric unit comprises two tetraanion SC4s (that are in the pinched cone conformation), two nine coordinate $Ce^{3+}$ centres in the distorted monocapped square antiprism geometry with six (Ce1) and seven (Ce2) water ligands in the inner sphere of the asymmetric unit, one G3 trication, two half-occupancy chloride ions and 21 disordered waters of crystallisation. The supermolecule in the asymmetric unit in complex **3** (Fig. 3a) has two of three methylimidazolium rings of G3 successfully confined within two independent SC4s assembled as a skewed capsule (approx. size 16 Å, Fig. 3a, as measured between SC4 lower-rim centroids). Owing to the guest's geometry, one of the imidazolium rings is positioned in a slantwise manner whilst the others are parallel to the two SC4 aromatic rings. However, both imidazolium moieties are not included deep within the SC4 cavities and are held weakly by $C\cdots\pi_{(phenyl)}$ interactions, with the shortest contacts found at 3.54 Å and 3.63 Å for the two end-capping SC4s. The inclusion of G3 is also augmented by additional stabilisation from C–H···O hydrogen bonding between the methylene bridge and SC4 sulfonate groups, with shortest contacts at 2.38 Å and 2.52 Å (corresponding C···O distances of 3.161(7) Å and 3.103(8) Å) for the two end-capping SC4s. The non-confined methylimidazolium group of G3 points towards the capsule seam and participates in hydrogen bonding with the surrounding SC4 sulfonate groups and the metal hydration sphere with calculated shortest C–H···O short contacts range at 2.79 and 2.69 Å respectively (corresponding C···O distances from 3.25 to 3.62 Å). The subtle differences between the N–C–C bond angles (angle of the arms) for the confined rings (111.3° and 111.9°) and non-confined ring (112.7°) are also noted.

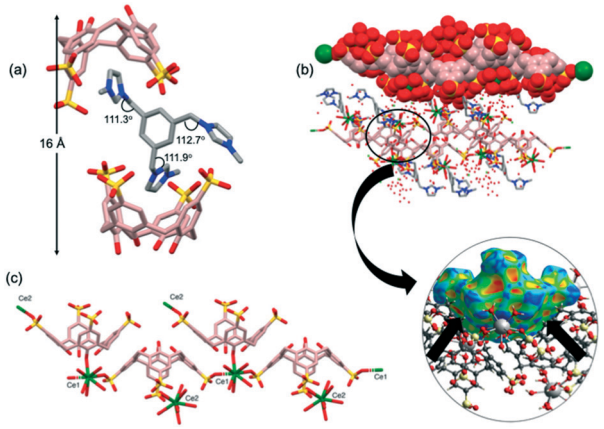


**Fig. 3** (a) Molecular capsule found in complex **3** with partially encapsulated G3 showing two imidazolium rings residing in SC4 cavities. (b) Partial space-filling illustrating the extended packing in complex **3** with Hirshfeld surface mapped with shape index to illustrate the π–π interactions shown in the inset. (c) Polymeric network of SC4s with cerium(III). H-Atoms omitted for clarity except in (b) and figures are not to scale.

The extended structure in complex **3** is rather complicated. Molecular capsules are arranged in regular manner and are separated by layers of divergent back-to-back SC4s, where they are held by intermolecular C–H···π interactions (close C···π distances are 3.56 Å and 3.57 Å). Adjacent SC4s are also in the closest association involving π–π stacking between the aromatic rings, $\pi_{(centroid)}\cdots\pi_{(centroid)}$ at 3.67 Å and 3.76 Å, and this hydrophobic interaction is evident on the Hirshfeld surface as judged from the presence of red and blue triangles on the surface and contributes 4.4% (Fig. 3b). The decomposition of the 2D fingerprint of complex **3** (Fig. 3b) reveals that the main interactions that hold the supermolecules together in the crystalline structure are reciprocal H···H (28.1%) and O···H/H···O (41.1%) interactions. C···H/H···C interaction involving the aromatics (corresponding to C–H···π) is also favored and contributes 18.0% to G3 Hirshfeld surface.

Inspection of the extended structure shows that one $Ce^{3+}$ coordination sphere comprises three O-atoms from three independent SC4 molecules (two from sulfonate groups, Ce1–$O11A_{(x,\ 1+y,\ z)}$ at 2.463(4) Å and Ce1–O31A at 2.463(4) Å, and one from a lower-rim hydroxyl group, $Ce1–O2B_{(x-1,\ y,\ z)}$ at 2.406(5) Å) and six aqua ligands (Ce–O distances ranging from 2.5142(3) to 2.6354(4) Å). The second nine-coordinate $Ce^{3+}$ ion bridges two independent SC4s through O-atoms of the sulfonate groups with Ce2–O21A and $Ce2–O11B_{(1-x,\ 1-y,1-z)}$ bond distances of 2.530(2) Å and 2.603(4) Å, respectively, with remaining coordination sites occupied by aqua ligands (Ce–O distances ranging from 2.4867(17) to 2.5308(16) Å). This results in a 2-D infinite polymeric network of capsules extending along the *bc*-plane (despite being finite along the *c*-direction), part of which is shown in Fig. 3c. Cerium(III) ions that are directly coordinated to SC4 sulfonate group further interact with adjacent SC4 upper-rims through hydrogen bonding, with Ce–O···O–S distances ranging from 2.582–2.836 Å.

**Structure of $[G4^{4+}\subset(SC4^{2-})_2]_2[Na^+]_2[Br^-]_2\cdot44H_2O$, 4**

The ternary system in complex **4** was found to crystallise in the orthorhombic crystal system with the space group $C222_1$. The asymmetric unit comprises one SC4 dianion in a pinched cone conformation, one half-populated G4 tetracation, one hydrated half-populated sodium cation, one half-populated bromide anion and twenty-two waters of crystallisation. As was the case in complex **3**, the G4 tetracation in **4** is partially encapsulated by the pinched cone SC4s (Fig. 4a), where only two of the four methylimidazolium rings are end-capped by the hosts (Fig. 4b). It is noteworthy that the capsular arrangement is sustained (approx. size of 17 Å, Fig. 4a, as measured from SC4 lower-rim centroids), in this case with the encapsulated G4 tetracation in a chair configuration, Fig. 4c. The G4 tetracation is disordered over a two-fold axis and has two methylimidazolium moieties on 1,2-position with respect to the benzene plane encapsulated by two independent SC4s, leaving the remaining two methylimidazolium moieties on the 4,5-positions unconfined (dihedral angles between the imidazolium rings and the benzene ring plane are between 111° to 112°). The two imidazolium rings that reside in the SC4 cavities have the methyl groups pointing towards the sulfonate groups with C⋯O distances at 3.23 and 3.48 Å.

It is also interesting to note that all the methylene bridges have close contacts with the SC4 sulfonate groups, forming hydrogen bonds with closest and farthest C⋯O distances of 3.05 Å and 3.34 Å, respectively. The two unconfined imidazolium rings have the methyl groups pointing towards the neighbouring SC4 sulfonate groups with C⋯O distances at 2.86 and 3.24 Å. Hirshfeld surface analysis revealed that a large percentage of the G4 $d_{norm}$ surface (53.3%) is contributed by the O⋯H/H⋯O interaction, followed by reciprocal H⋯H and C⋯H/H⋯C interactions, which contribute 22.0% and 13.1%, respectively.

The molecular capsules in the extended structure are arranged such that they form the common alternating hydrophilic and hydrophobic bilayer structure; the calculated bilayer thickness is ~9.4 Å (Fig. 4b) and the interlayer distance is ~16 Å. The SC4 aromatic rings participate in offset π-stacking and C–H⋯π interaction with the closest C⋯π distance at 3.69 Å and closest $\pi_{(centroid)}\cdots\pi_{(centroid)}$ distance at 3.77 Å. These interactions represent ~13% of all the intermolecular interactions involving SC4 in the structure as summarized by the Hirshfeld surface analysis, Fig. S2.† The presence of blue and red triangles are visible on the SC4 Hirshfeld surface when mapped over curvedness, Fig. 4d. The structure is heavily hydrated and water molecules (disordered) are in close proximity to the oxygen species of SC4 and participate in hydrogen bonding with SC4 and amongst themselves with O⋯O ranging from 2.53 to 2.84 Å. Finally, sodium ions participate in hydrogen bonding with O-atoms of the SC4 sulfonate (Na1⋯O34 = 2.96(3) Å), hydroxyl groups (Na1⋯O2 = 2.78(2) Å) and surrounding water molecules (Na⋯O = 2.696 to 3.236 Å).

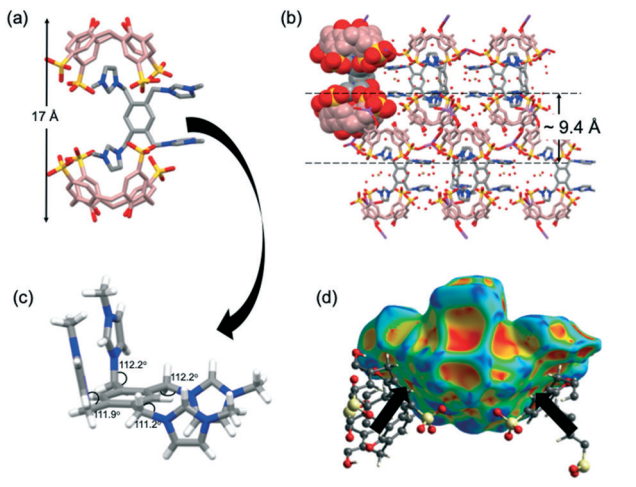


Fig. 4 (a) Molecular capsule formed in complex **4** with G4 partially encapsulated. (b) Partial space-filling illustrating the extended packing in complex **4**. (c) Chair conformation of G4. (d) Hirshfeld surface mapped with shape index to illustrate the π–π interactions. H-Atoms were omitted for clarity except in (c) and (d), and figures are not to scale.

## Conclusions

Four crystal structures of water-soluble SC4 with a series of mono and multicharged imidazolium salts along with lanthanide(III) cations were carefully investigated using X-ray crystallographic analysis. Driven by the electrostatic interaction, the preferential binding towards the five-membered species by SC4 was evident, affording the formation of 2:1 host–guest complexes in all cases. All complexes showed that the guest molecules are accommodated in the molecular capsule comprising two opposing SC4 molecules stabilised by multiple hydrogen bonds and weak C–H⋯π interactions. However, the interplay of the guest molecule is rather different in each complex, a feature that appears to be attributable to its size. The smaller 1-methylimidazolium, G1 and 3,3′-(1,4-phenylenebis(methylene))bis(1-methylimidazolium), G2, guests fit snugly in the core of the molecular capsule, whilst the larger 3,3′,3″-(benzene-1,3,5-triyltris(methylene))tris(1-methylimidazolium), G3 and 3,3′,3″,3‴-(benzene-1,2,4,5-tetrayltetrakis(methylene))tetrakis(1-methylimidazolium), G4, species drive partial encapsulation, where only two of the three or four respective methylimidazolium rings are successfully end-capped by SC4s. Although an extensive array of inclusion complexes involving imidazolium and SC4 have been reported in the presence of phosphonium cations, the structures reported herein describe corresponding self-assembly behaviours in its absence. Hirshfeld surface analysis was utilised to discern the dominant intermolecular interactions that contribute to the overall cohesion of all the species in the solid-state. The extended packing for complexes **2** to **4** suggest that SC4 molecules can preserve the bilayer arrangement persistently, however for complex **1**, a hexagonal array formed

 

with the presentation of large hydrophilic channels. This shows that the self-assembly of SC4 in depends strongly on the nature of the imidazolium moieties, and that the absence of large hydrophobic cations (*e.g.* phosphonium) in the hydrophobic layer gives rise to dramatically different assembly behaviours. Future work will focus on the modification of the multicharged polycations with different functionality including saturated amines (both aliphatic and cyclic) and host–guest interactions with SC4 and larger calixarene analogues.

## Author contributions

The authors indicated in the parentheses made substantial contributions to the following tasks of research: initial conception and design (IL); synthesis (IL); provision of resources (IL, SJD); collection of data (ANS, CLC); analysis and interpretation of data (IL, ANS, CLC, SJD); writing and revision of paper (IL, ANS, SJD).

## Conflicts of interest

There are no conflicts to declare.

## Acknowledgements

We thank the Ministry of Higher Education Malaysia for financial support from Fundamental Research Grant Scheme (FRGS/1/2018/STG07/MUSM/03/1), and the EPSRC for studentship support for CLC. We also thank Monash University Malaysia, Heriot-Watt University, and The University of Western Australia for supporting this work.

## Notes and references

1 J. Kang, G. Hilmersson, J. Santamaria and J. Rebek, Jr., *J. Am. Chem. Soc.*, 1998, **120**, 3650.
2 C. L. D. Gibb and B. C. Gibb, *J. Am. Chem. Soc.*, 2004, **126**, 11408.
3 H. Gan and B. C. Gibb, *Chem. Commun.*, 2013, **49**, 1395.
4 L. Turunen, U. Warzok, C. A. Schalley and K. Rissanen, *Chem*, 2017, **3**, 861.
5 U. Warzok, M. Marianski, W. Hoffmann, L. Turunen, K. Rissanen, K. Pagel and C. A. Schalley, *Chem. Sci.*, 2018, **9**, 8343.
6 M. M. Conn and J. Rebek, Jr., *Chem. Rev.*, 1997, **97**, 1647.
7 R. G. Chapman, G. Olovsson, J. Trotter and J. C. Sherman, *J. Am. Chem. Soc.*, 1998, **120**, 6252.
8 L. R. MacGillivray and J. L. Atwood, *Nature*, 1997, **389**, 469.
9 O. D. Fox, N. K. Dalley and R. G. Harrison, *J. Am. Chem. Soc.*, 1998, **120**, 7111.
10 B. Olenyuk, M. D. Levin, J. A. Whiteford, J. E. Shield and P. J. Stang, *J. Am. Chem. Soc.*, 1999, **121**, 10434.
11 O. D. Fox, M. G. B. Drew and P. D. Beer, *Angew. Chem.*, 2000, **112**, 140.
12 M. Ziegler, J. L. Brumaghim and K. N. Raymond, *Angew. Chem.*, 2000, **112**, 4285.
13 T. N. Parac, M. Scherer and K. N. Raymond, *Angew. Chem.*, 2000, **112**, 1288.
14 A. J. Terpin, M. Ziegler, D. W. Johnson and K. N. Raymond, *Angew. Chem.*, 2001, **113**, 161.
15 R. Wyler, J. de Mendoza and J. Rebek, Jr., *Angew. Chem., Int. Ed. Engl.*, 1993, **32**, 1699.
16 J. M. Rivera, T. Martin and J. Rebek, Jr., *Science*, 1998, **279**, 1021.
17 S. Liu and B. C. Gibb, *Chem. Commun.*, 2008, 3709.
18 L. Bonomo, E. Solari, G. Toraman, R. Scopelliti, M. Latronico and C. Floriani, *Chem. Commun.*, 1999, 2413.
19 G. J. Lumetta, R. D. Rogers and A. S. Gopalan, *Calixarenes for Separations*, Oxford University Press, 2000.
20 A. Casnati and R. Ungaro, in *Calixarenes in Action*, ed. L. Mandolini and R. Ungaro, Imperial College Press, London, 2000.
21 E. S. Español and M. M. Villamil, *Biomolecules*, 2019, **9**, 90.
22 I. Ling and C. L. Raston, *Comprehensive Supramolecular Chemistry II*, 2017, pp. 19–73.
23 I. Ling and C. L. Raston, *Coord. Chem. Rev.*, 2018, **375**, 80.
24 I. Ling, Y. Alias and C. L. Raston, *New J. Chem.*, 2010, **34**, 1802.
25 K. Ganesan and Y. Alias, *Int. J. Mol. Sci.*, 2008, **9**, 1207.
26 I. Ling, A. N. Sobolev, S. L. Loh, G. F. Turner and S. A. Moggach, *CrystEngComm*, 2020, **22**, 5539.
27 J. Vicens and V. Böhmer, *Calixarenes: A Versatile Class of Macrocyclic Compounds*, Springer Science & Business Media, 2012.
28 G. M. Sheldrick, *Acta Crystallogr., Sect. C: Struct. Chem.*, 2015, **71**, 3.
29 A. L. Spek, *Acta Crystallogr., Sect. C: Struct. Chem.*, 2014, **71**, 9.
30 I. Ling, A. N. Sobolev and C. L. Raston, *CrystEngComm*, 2016, **18**, 4929.
31 I. Ling, Y. Alias, A. N. Sobolev and C. L. Raston, *CrystEngComm*, 2010, **12**, 1869.
32 P. R. Spackman, M. J. Turner, J. J. McKinnon, S. K. Wolff, D. J. Grimwood, D. Jayatilaka and M. A. Spackman, *J. Appl. Crystallogr.*, 2021, **54**, 1006.
33 I. Ling, Y. Alias, A. N. Sobolev and C. L. Raston, *Cryst. Growth Des.*, 2009, **9**, 4497.